PNAS RESEARCH ARTICLE | IMMUNOLOGY AND INFLAMMATION OPEN ACCESS

Attenuation of relapsing fever neuroborreliosis in mice by IL-17A blockade

Meihui Cheng[a,1], Jingwen Xu[a,1], Kaiyun Ding[a], Jing Zhang[a], Wei Lu[a], Jiansheng Liu[a], Jiahong Gao[a], Kishore R. Alugupalli[b], and Hongqi Liu[a,2]

Edited by Lawrence Steinman, Stanford University, Stanford, CA; received March 29, 2022; accepted September 6, 2022

Relapsing fever due to *Borrelia hermsii* is characterized by recurrent bacteremia episodes. However, infection of *B. hermsii*, if not treated early, can spread to various organs including the central nervous system (CNS). CNS disease manifestations are commonly referred to as relapsing fever neuroborreliosis (RFNB). In the mouse model of *B. hermsii* infection, we have previously shown that the development of RFNB requires innate immune cells as well as T cells. Here, we found that prior to the onset of RFNB, an increase in the systemic proinflammatory cytokine response followed by sustained levels of IP-10 concurrent with the CNS disease phase. RNA sequencing analysis of the spinal cord tissue during the disease phase revealed an association of the interleukin (IL)-17 signaling pathway in RFNB. To test a possible role for IL-17 in RFNB, we compared *B. hermsii* infection in wild-type and IL-17A$^{-/-}$ mice. Although the onset of bacteremia and protective anti-*B. hermsii* antibody responses occurred similarly, the blood-brain barrier permeability, proinflammatory cytokine levels, immune cell infiltration in the spinal cord, and RFNB manifestations were significantly diminished in IL-17A$^{-/-}$ mice compared to wild-type mice. Treatment of *B. hermsii*-infected wild-type mice with anti-IL-17A antibody ameliorated the severity of spinal cord inflammation, microglial cell activation, and RFNB. These data suggest that the IL-17 signaling pathway plays a major role in the pathogenesis of RFNB, and IL-17A blockade may be a therapeutic modality for controlling neuroborreliosis.

neuroborreliosis | *Borrelia hermsii* | interleukin-17 | relapsing fever | inflammation

Significance

Spirochetes of the genus *Borrelia* can spread to various organs including the central nervous system. The neurological disease manifestations in these bacterial infections are commonly referred as neuroborreliosis. Currently, long-term antibiotic treatment is the only the United States Food and Drug Administration-approved option for those suffering from neuroborreliosis. Using *Borrelia hermsii* infection in mice, we have previously established a relapsing fever neuroborreliosis model. In this model, we found that the induction of interleukin (IL)-17A signaling plays a major role in the pathogenesis of relapsing fever neuroborreliosis. We show that anti-IL-17A antibody treatment can ameliorate the pathology. Our data suggest that IL-17A blockade may be a therapeutic strategy for controlling relapsing fever neuroborreliosis.

Neuroborreliosis is a disorder of the central nervous system (CNS) caused by a systemic infection of spirochetes of the genus *Borrelia* including *B. burgdorferi* and *B. hermsii* (1, 2). Infection with *B. burgdorferi,* an agent of Lyme disease, typically causes an expanding skin lesion known as *erythema migrans*, which occurs at the site of the tick bite (3). On the other hand, infection with *B. hermsii*, an agent of relapsing fever, is characterized by recurrent bacteremic episodes (4, 5). If untreated, these spirochetes can disseminate into several tissues, including the CNS, and can produce a wide range of disease manifestations. In the case of Lyme neuroborreliosis (LNB), the common clinical features are lymphocytic meningitis, cranial neuritis, or radiculoneuritis and facial paralysis (6, 7). While most *B. burgdorferi*-infected patients recover with antibiotic treatment, ∼15% of infected individuals experience long-term neurological and psychological symptoms that are unresponsive to antibiotics (8–10).

The ratio of CNS disease complications in relapsing fever patients is similar to that in Lyme patients (11). The incidence and characteristics of relapsing fever neuroborreliosis (RFNB) in humans varies with the relapsing fever *Borrelia* species as well as the immune status of the host (1). For example, in the case of *B. recurrentis*, the incidence of CNS complications can be as high as 40% (4). Recently, *B. miyamotoi* was shown to be responsible for the RFNB in a patient undergoing B cell depletion therapy for non-Hodgkin lymphoma (12). In the murine model, *B. turicatae* was shown to invade the CNS of immunodeficient mice in a serotype-dependent manner and vestibular dysfunction is one of the prominent neurological manifestations (13, 14). The murine models for neurological involvement during *B. hermsii* infections were characterized mainly by the presence of bacteria in the CNS and meningitis in immunodeficient mice (15, 16). However, using the *B. hermsii* strain DAH, an isolate from a relapsing fever patient, we found that immunocompetent wild-type C57BL/6 mice, when infected with the strain DAH, exhibit a high incidence of CNS disease manifestations (17). Furthermore, we found infiltration of many T cells into the lumbar region of the spinal cord of *B. hermsii*-infected mice. Additionally, we found up-regulation of MHC II and CD80 on infiltrating macrophages and resident microglial cells, suggesting roles for T cell and innate immune cells in the pathogenesis of RFNB. Indeed, *B. hermsii* infection did not induce CNS disease manifestations in T cell-deficient (TCR-βxδ$^{-/-}$) mice, although it resulted in bacteremia comparable to that in wild-type mice. Moreover, the

Author contributions: H.L. designed research; M.C., J.X., K.D., J.Z., W.L., J.L., and J.G. performed research; M.C., J.X., and J.G. analyzed data; M.C., K.R.A., and H.L. wrote the paper; K.R.A. contributed to the development of the relapsing fever neuroborreliosis; provided critical advice on the manuscript; and H.L. contributed to the development of the relapsing fever neuroborreliosis.

The authors declare no competing interest.

This article is a PNAS Direct Submission.

See online for related content such as Commentaries.

[1]M.C. and J.X. contributed equally to this work.

[2]To whom correspondence may be addressed. Email: lhq@lmbcams.com.cn.

This article contains supporting information online at http://www.pnas.org/lookup/suppl/doi:10.1073/pnas.2205460119/-/DCSupplemental.

Published October 10, 2022.

infiltration of immune cells into the spinal cord of TCR-βxδ$^{-/-}$ mice was reduced, and the resident microglial cells were not activated. Histopathological analysis of lumbar sections of the spinal cord confirmed severe inflammation in wild-type but not in TCR-βxδ$^{-/-}$ mice (17).

Immunopathogenesis is an important player in the infection-induced neurological diseases (18, 19). Currently, long-term antibiotic treatment remains the only US Food and Drug Administration-approved option for those suffering from LNB or RFNB (6). A better understanding of neuroborreliosis will permit the identification of new therapeutic targets for an improved treatment. Interleukin 17 (IL-17) plays an important role in several CNS-associated diseases (20) as well as autoimmune diseases (21). IL-17 was initially recognized to function by activation of neutrophils and their migration to the inflammation site (22). For example, neutralization of IL-17 by antibody prevents the infiltration of neutrophils and protects against ischemic stroke (23). Therefore, IL-17 is recognized as a potential therapeutic target for several CNS diseases (24). Indeed, several monoclonal antibodies against IL-17 or its receptor have been evaluated in clinical studies of autoimmune diseases.

Components derived from pathogens can stimulate host cells to produce IL-17 that interacts with vascular endothelial cells to dissociate tight junctions and increase the permeability of the blood-brain barrier (BBB). IL-17 can activate microglia and astrocytes to produce inflammatory cytokines and chemokines that can recruit inflammatory cells from the periphery into the CNS thereby exacerbating CNS manifestations (25). *Borrelia* can induce the production of IL-17 from the host cells in vitro (26, 27). A correlation of increased levels of several cytokines and chemokines including IL-17 were observed in individuals experiencing LNB (28). Since we have an established *B. hermsii* infection model of RFNB (17), in the present study we tested the role of IL-17. We found that the lack of IL-17 or IL-17 blockade decreases the severity of RFNB, suggesting that IL-17 signaling can be a potential target for treating neuroborreliosis.

Results

Neuroborreliosis Is Associated with the Systemic Inflammation in *Borrelia hermsii*-Infected Mice. To investigate the pathogenesis of RFNB, we infected the immunocompetent C57BL/6 mice with *B. hermsii* strain DAH (29) that is fully virulent in wild-type mice (17). As expected, recurrent bacteremia was developed, and *B. hermsii*-specific antibody responses were induced (Fig. 1*A* and *SI Appendix*, Fig. S1 *A–C*). On day 8 post infection, mice began to show CNS complications, such as tail weakness, followed by hind limb weakness and even paralysis, and the incidence of symptoms reached 100% (Fig. 1 *B* and *C*) as reported previously (17). To further understand the pathogenesis of RFNB, we measured a panel of cytokines and chemokines associated with innate immune cells and T cells and evaluated the temporal correlation of systemic inflammation in C57BL/6 mice infected with *B. hermsii*. Prior to the induction of the CNS manifestations, high levels of the cytokine IL-6 as well as chemokines MIP-1β and MCP-1 were induced, suggesting the activation of monocytes and macrophages during this phase (Fig. 1*D*). Interestingly, IP-10, known to attract a variety of immune cells including T cells and dendritic cells, and to promote T cell adhesion to endothelial cells, is induced throughout the *B. hermsii* infection phase. In the spinal cords of infected animals, satellitosis was observed on 7 dpi and 14 dpi (Fig. 1*E*). The activation marker CD68 of inflammatory cell was significantly enhanced on 14 dpi as compared with that on 0 and 7 dpi (Fig. 1*F*). mRNA levels of *IL-6*, *IL-8*, and *TNF*-α significantly increased in the spinal cords on 14 dpi (*SI Appendix*, Fig. S1*D*). Pathological changes were also observed in spleens of *B. hermsii*-infected animals. On 7 dpi, megakaryocytes and infiltration of inflammatory cells were observed in the spleens, followed by spleen congestion and influx of inflammatory cells on 14 dpi (*SI Appendix*, Fig. S1*E*). Together, these data suggest that systemic inflammation is associated with neurological inflammation and the CNS complications.

The IL-17 Signaling Pathway Is Associated with Neuroborreliosis. To further explore the factors associated with the pathogenesis of RFNB, we performed RNA sequencing (RNA-seq) analysis of the spinal cords isolated from C57BL/6 mice on 14 d post infection. Compared to uninfected mice, 1,525 genes were differentially expressed in the spinal cords of *B. hermsii*-infected mice, of which 1,487 genes were up-regulated and 38 genes were down-regulated (Fig. 2*A*). To validate the results from the RNA-seq, we analyzed a subset of genes that are either up-regulated or down-regulated (Fig. 2*B*) by real-time quantitative reverse transcription PCR (qRT-PCR) (Fig. 2*C*). Kyoto Encyclopedia of Genes and Genomes (KEGG) pathway analysis of RNA-seq data showed that multiple innate immune and inflammatory signaling pathways including IL-17 were activated in the spinal cord during *B. hermsii*-infection (Fig. 2*D*). Gene Set Enrichment Analysis (GSEA) confirmed significant enrichment of genes related to the IL-17 signaling pathway (Fig. 2*E*). These data suggest that the IL-17 signaling pathway is involved in the development of RFNB.

To directly test the involvement of IL-17 signaling in the pathogenesis of RFNB, we compared *B. hermsii* infection in mice sufficient or deficient in IL-17A (IL-17A$^{-/-}$), the prototype member of the IL-17 cytokine family (24). We have previously shown that control of *B. hermsii* infection is mediated by a T cell-independent immunoglobulin M (IgM) response (17). Here we found that the levels of *B. hermsii* bacteremia as well as the anti-*B. hermsii* response in IL-17A$^{-/-}$ mice were comparable to those in wild-type mice (*SI Appendix*, Fig. S2 *A* and *B*), indicating that the deficiency of IL-17A had no effect on the severity of bacterial burden or antibody-mediated control. However, the severity and the incidence of the CNS disease in IL-17A$^{-/-}$ mice were significantly limited as compared with those in the wild-type mice (Fig. 3 *A* and *B*).

We have previously shown an association of a massive infiltration of macrophages, B cells, CD4^{+} T cells, CD8^{+} T cells, and natural killer (NK) cells with RFNB (17). We also found that in the absence of T cells, neither infiltration nor inflammatory lesions are generated in the spinal cords of *B. hermsii*-infected mice (17). Circulating IL-17 promotes BBB disruption by altering expressions of tight junctions and cell-adhesion molecules on endothelial cells (30). Since the severity of the RFNB is attenuated in IL-17 A$^{-/-}$ mice, we investigated the effects of IL-17 deficiency on the integrity of the blood-spinal cord barrier (BSCB) by analysis of the tight junction protein ZO-1 and vascular marker CD31. We observed that ZO-1 localization in the spinal cord was significantly reduced in *B. hermsii* infected wild-type but not IL-17A$^{-/-}$ mice (Fig. 3 *C* and *D* and *SI Appendix*, Fig. S2 *C* and *D*), suggesting that the lack of IL-17 signaling could protect BSCB integrity during *B. hermsii* infection. Analysis of proinflammatory cytokines in the spinal cords showed that mRNA levels of *IL-6*, *IL-8*, and *TNF*-α were significantly reduced in infected IL17A$^{-/-}$ mice compared with those in wild-type mice (Fig. 3*E*). Although satellitosis and infiltration of inflammatory cells were observed in the spinal

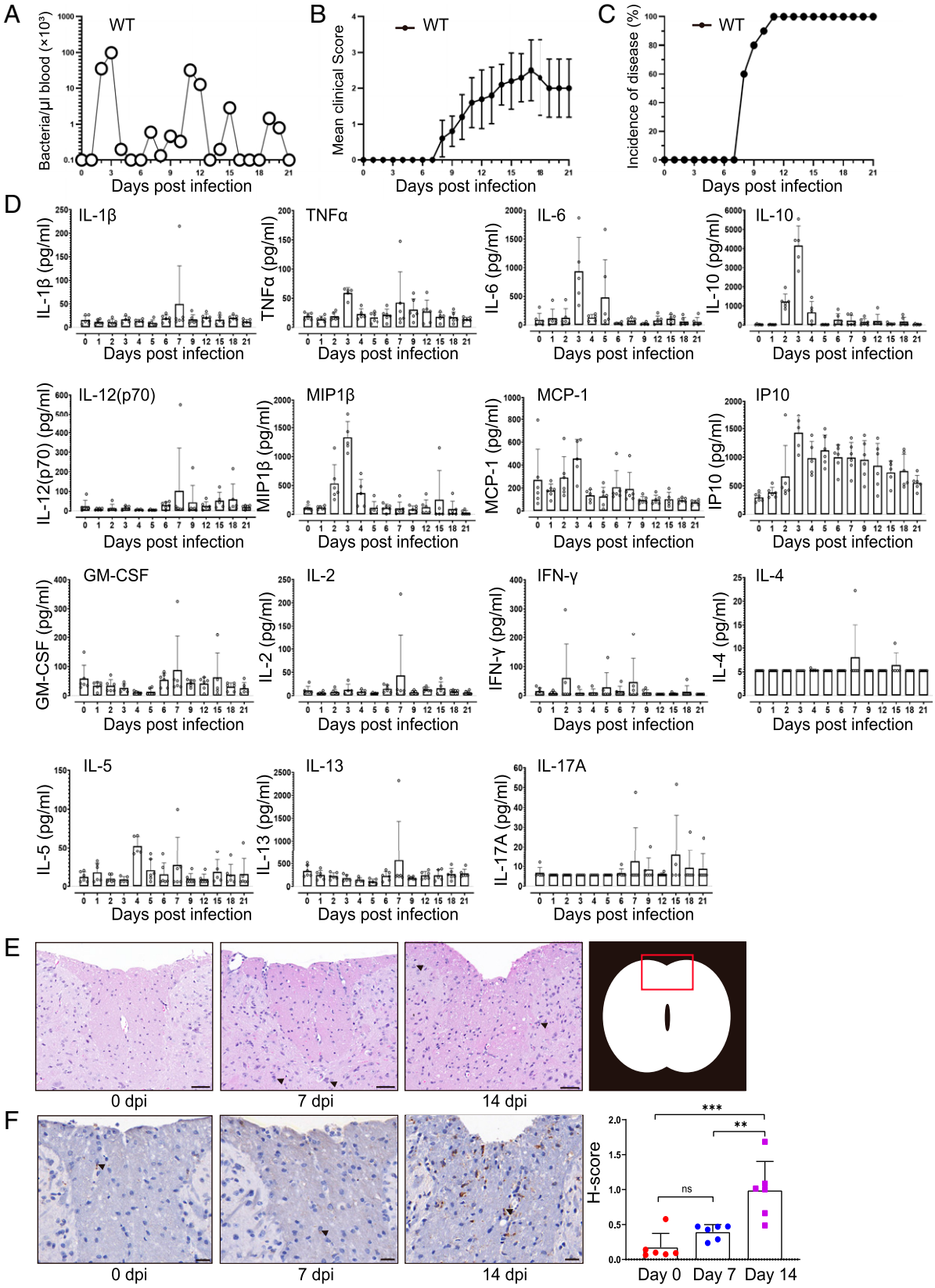

Fig. 1. Systemic inflammation and neuroborreliosis during *B. hermsii* infection. (*A–C*) Wild-type C57BL/6 mice (n = 10) were infected intraperitoneally (i.p.) with 5 × 10^4 spirochetes of *B. hermsii* strain DAH. Blood was collected daily until day 21 for monitoring bacteremia (a representative plot from one mouse) (*A*), clinical score (*B*), and incidence of CNS disease (*C*) (as described in *Materials and Methods*). (*D*) At the indicated time points, serum samples from infected mice were harvested for measurement of inflammatory cytokines by Luminex. Data are represented as mean ± SD (n = 6 for each time point). (*E* and *F*) Spinal cords of wild-type mice were collected on 0-, 7- and 14-d post infection (n = 6 for each time point) for histological analysis via H&E staining or immunohistochemistry staining. The representative pathological changes in spinal cords of H&E-stained specimens were indicated by arrows (*E*). The representative staining of CD68 was indicated by arrows (*F*). The activation of inflammatory cells was quantified as H-score (as described in *Materials and Methods*) (*F*). All data are represented as mean or mean ± SD. Where applicable, data were analyzed via ordinary one-way ANOVA. *P < 0.05, **P < 0.01, and ***P < 0.001 and ns means no significant difference ($P \geq 0.05$). (Scale bars for *E* and *F*: 50 μm.)

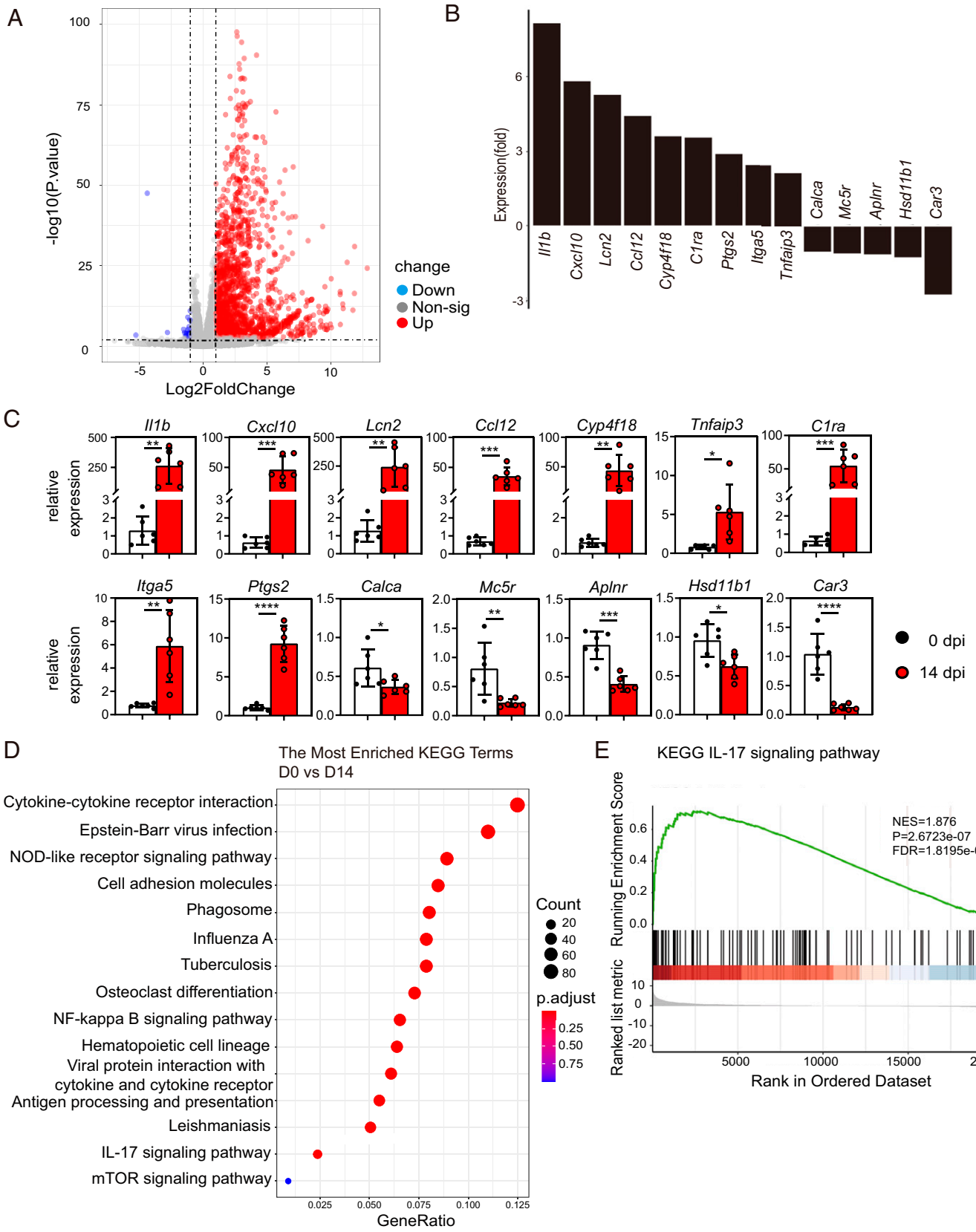

Fig. 2. Activation of inflammation-associated signal pathways during *B. hermsii* infection. Wild-type C57BL/6 mice were infected i.p. with 5×10^4 spirochetes of *B. hermsii* and at days 0 and 14 post inoculation, spinal cords were harvested for RNA-seq analysis ($n = 4$ for each time point). (*A*) Volcano plot representing differential gene expression on 0- and 14-d post infection. A subset of differentially expressed genes in RNA-seq (*B*) was validated by qRT-PCR (*C*). (*D*) Enrichment of regulatory pathways involved in *B. hermsii* infection was analyzed via KEGG. (*E*) Involvement of IL-17 signaling pathway during *B. hermsii* infection was revealed by GSEA.

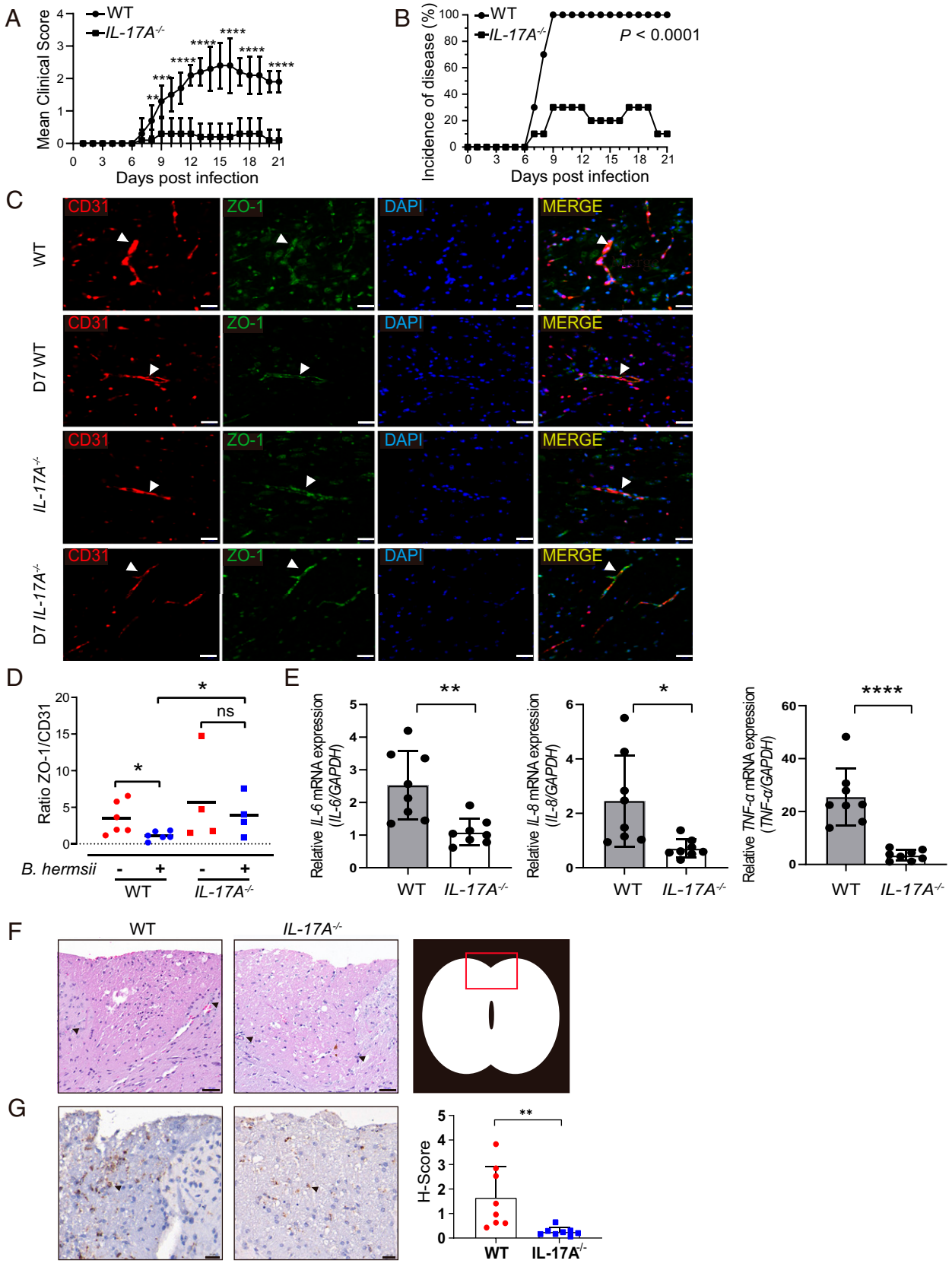

Fig. 3. IL-17 signal plays a major role in the induction of relapsing fever neuroborreliosis. (*A* and *B*) Wild-type (WT) or IL-17A$^{-/-}$ mice (n = 10 per group) were infected i.p. with 5 × 10^4 *B. hermsii* strain DAH. The disease severity (*A*) and incidence (*B*) of the disease manifestations were monitored for 21 d. (*C*) Wild-type (WT) (n = 6) or IL-17A$^{-/-}$ mice (n = 4) were euthanized on day 7 post infection and spinal cords were collected for detection of ZO-1 (green) and CD31 (red) by immunofluorescence assay. (*D*) The ratio of positive area of ZO-1 over CD31 was calculated and each dot represents an individual mouse. (*E*) On day 14 post infection, *IL-6*, *IL-8*, and *TNF*-α mRNA expression in the spinal cord of wild-type or IL-17A$^{-/-}$ mice (n = 8 per group) was quantified by qRT-PCR. (*F* and *G*) Spinal cords of wild-type and IL-17A$^{-/-}$ (n = 8 per group) mice were analyzed for histological change as those in Fig. 1 *E* and *F*. All data are represented as mean or mean ± SD. Where applicable, data were analyzed via two-tailed unpaired Student's t test. *P < 0.05, **P < 0.01, ***P < 0.001 and ns means no significant difference ($P \geq 0.05$). (Scale bars for *C*, *F*, and *G*: 50 μm.)

cords of both wild-type and IL-17A$^{-/-}$ mice (Fig. 3*F*), the activation of inflammatory cells was significantly lower in IL-17A$^{-/-}$ mice compared with that of wild-type mice (Fig. 3*G*). These results demonstrate that IL-17 signaling plays a prominent role in the pathogenesis of RFNB.

Blocking IL-17A Attenuates CNS Disease Manifestations Induced by *B. hermsii* Infection. Since IL-17A is involved in RFNB (Figs. 2 and 3), we speculated that IL-17A signaling might be a possible therapeutic target for this disease. To test this, we intraperitoneally administered anti-IL-17A antibody into wild-type mice and then infected them with *B. hermsii*. This treatment did not affect the development of bacteremia or the induction of *B. hermsii*-specific IgG and IgM antibodies (*SI Appendix*, Fig. S3 *A* and *B*). However, the treatment with anti-IL-17A antibody significantly reduced the CNS disease manifestations and the incidence of this CNS disease (Fig. 4 *A* and *B*). Furthermore, we found that anti-IL-17A antibody treatment mitigated the histopathology of the spinal cord in *B. hermsii*-infected mice (Fig. 4*C*). These findings suggest that IL-17A could be a potential therapeutic target for controlling RFNB.

To further explore the therapeutic mechanism of anti-IL-17 antibody, we firstly analyzed inflammation in the spinal cords of infected animals. The inflammatory cytokines *IL-6*, *IL-8*, and *TNF*-α were significantly decreased in anti-IL-17A antibody-treated animals as compared with those in untreated animals (Fig. 4*D*). Strikingly, this decrease of inflammatory cytokine was not observed in the spleen of treated mice (*SI Appendix*, Fig. S3*C*). We then investigated the cellular mechanism involved in anti-IL-17 antibody treatment using immunofluorescence analysis of the microglia marker Iba-1 and activation marker CD68 in the spinal cord. The percentage of Iba-1^{+}CD68^{+} cells in the spinal cord was significantly reduced in mice treated with anti-IL-17A antibody as well as in IL-17A$^{-/-}$ mice as compared with that in untreated but infected wild-type mice (Fig. 4 *E* and *F*), indicating that blockade of IL-17 signaling prevented activation of microglia in the CNS. These data suggest that targeting IL-17 could improve neurological complications by reducing the inflammation in the CNS during RFNB.

Discussion

Complications of the CNS can occur in a wide range of infections, which may lead to permanent neurological deficits in survivors (31). Neuroinflammation is a prominent factor for the most neurological manifestations (32). The presence of spirochete in the CNS is one of important index for the induction of neuroinflammation (1, 2). In the murine model of Lyme disease, *B. burgdorferi* colonizes the dura mater and induces inflammation in the central nervous system (33). However, in the *B. hermsii*-infected neuroborreliosis, we were unable to detect the spirochete by current methods possibly due to the limitation of sensitivity and very low number of spirochetes. It is possible that the RFNB could also be mediated by aseptic inflammation in the CNS. In fact, aseptic meningitis is also described in relapsing fever patients (34). Biomarkers for CNS disease are usually identified by analysis of cerebrospinal fluid in clinical samples (27). *Borrelia* is known to induce the production of IL-17 (26, 27). Since we have established a murine model of CNS disease manifestations as well as pathology in immunocompetent mice (17), in the present study, we were able to identify the impact of IL-17 in the pathogenesis of RFNB.

IL-17, as an inflammatory and regulatory cytokine, has been investigated in the physiological and pathological conditions for nearly 30 y (24). The effects of IL-17, a double-edged sword, are beneficial to wound healing, epithelial proliferation, microbiota homeostasis, inflammation to combat infection, but also involved in the pathogenesis of multiple autoimmune diseases, chronic degenerating diseases, chronic inflammation, and diabetes-associated inflammation (35). These effects are determined by the amount of IL-17, status of its responding cells and microenvironment. At present, there are three antibodies against IL-17 being used in clinical therapy for autoimmune diseases (36).

There are six members in the IL-17 family (IL-17A–IL-17F) and each appears to have a distinct function (37). IL-17A is the most studied immuno-regulatory inflammatory cytokine. In this study, we blocked the IL-17A signaling by the administration of a neutralization antibody against IL-17A to attenuate the disease severity (Fig. 4). The main cell types that produce IL-17 are CD4^{+} T cells (Th17), followed by CD8^{+} T cells (Tc17) and innate immune cells such as NK T cells, ILC3 cells, nTh17 cells (38), microglia (39), and neutrophils (40). Furthermore, microglia and neutrophils also express receptors for IL-17. Therefore, IL-17 secreted by microglia or neutrophils can activate themselves via an autocrine loop to further produce inflammatory cytokines IL-6, IL-1β, TNF-α and MIP-2 (39). Here, we observed an increased number of Iba-1^{+}CD68^{+} cells in the spinal cord of mice with *Borrelia*-induced neurological symptoms (Fig. 4), suggesting the activation of microglia. Notably, treatment with anti-IL-17A antibody and a deficiency of IL-17A blocked the activation of microglia (Fig. 4). However, more studies are needed to understand the intrinsic or extrinsic effects of IL-17 signaling on microglia.

CD4^{+} T cells significantly contribute to pathogen-specific adaptive immune responses via the production of effector cytokines (e.g., interferon [IFN]-γ and IL-17). For example, Th17 cells play critical roles in protective immunity against extracellular pathogens *Klebsiella pneumoniae*, *Citrobacter rodentium*, and *Candida albicans* as well as intracellular bacteria like *Listeria monocytogenes*, *Salmonella enterica*, and *Mycobacterium tuberculosis* (41). However, Th17 cells are not expected to play a role in host defense against *B. hermsii*, since we have shown that T cell-independent IgM responses mediated by B1b cells are sufficient for controlling *B. hermsii* infection (42, 43). Consistent with a lack of a requirement for T cells in controlling *B. hermsii*, genetic ablation of IL-17A or antibody-mediated depletion of IL-17A has no impact on the protective antibody response against *B. hermsii* (*SI Appendix*, Fig. S2 *A* and *B*). Since T cells are required for the pathogenesis of RFNB (17), it is possible that they contribute to disease progression by either producing IL-17 or other upstream and downstream factors of the IL-17 signaling pathway. For example, *B. hermsii* infection results in production of high levels of systemic IL-6 prior to the RFNB induction phase (44) (Fig. 1*D*). It is known that IL-6 is one of the prominent cytokines for promoting the development of Th17 cells via the STAT3 pathway (45). It has been reported that IL-17 synergizes with IL-6 to enhance the production of IL-6 by the astrocytes via a positive feedback loop (46). We found that IL-6 transcripts were induced in the spinal cord of *B. hermsii*-infected wild-type mice (*SI Appendix*, Fig. S1*D*). This induction was significantly reduced in the wild-type mice treated with anti-IL-17 antibody (Fig. 4*D*) or in mice deficient in the IL-17A (Figs. 3*E* and 4*D*). Interestingly, the increase of IL-6 transcripts was not observed in the spleen during the RFNB phase (*SI Appendix*, Fig. S3*C*). This suggests that IL-6 may be synergizing with IL-17A in the astrocytes or other cells of the CNS to generate an exaggerated inflammation by the infiltrated T cells in the spinal cord, but not by those T cells

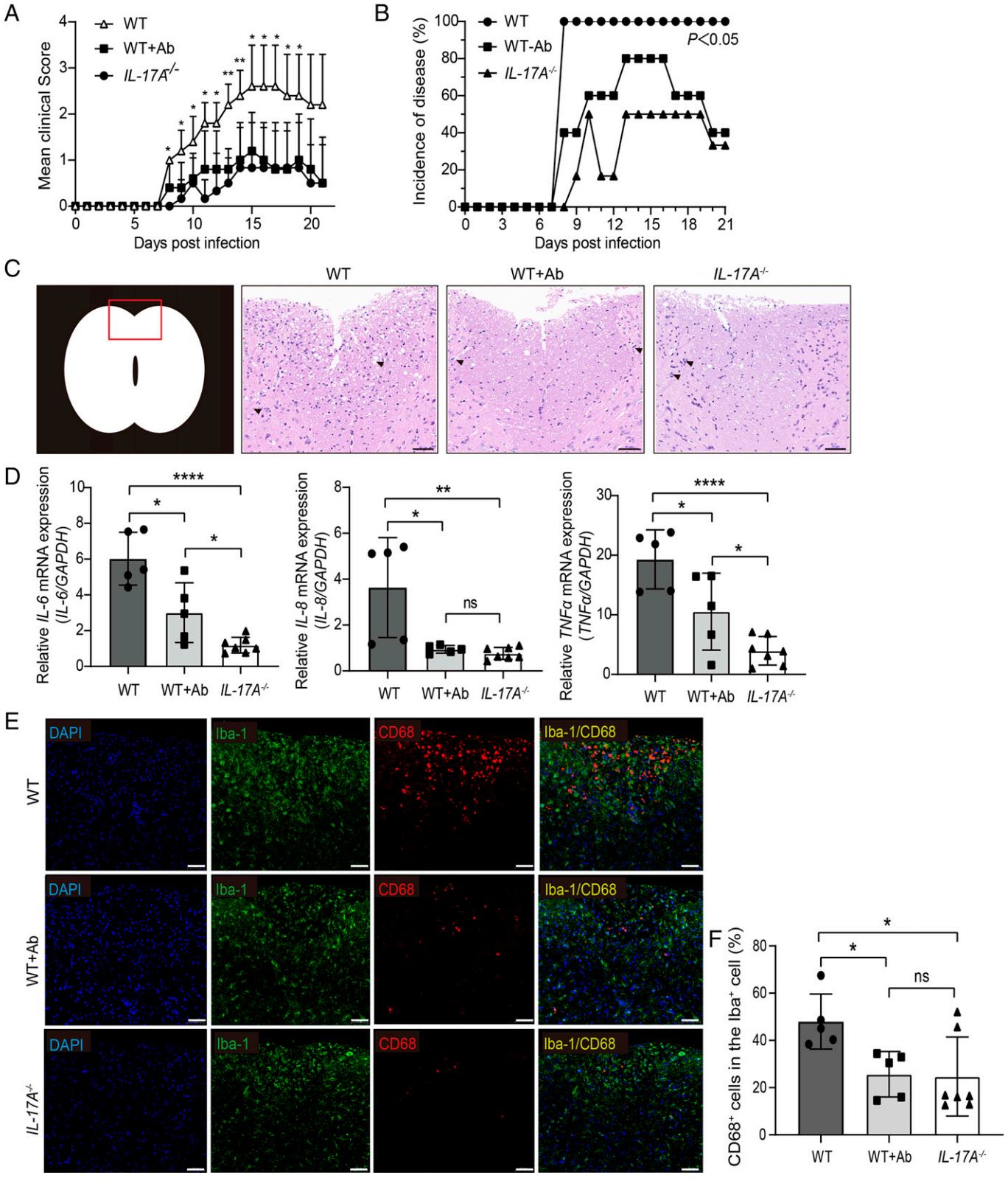

Fig. 4. Blocking IL-17A ameliorates neuroborreliosis induced by *B. hermsii* infection. (*A* and *B*) Wild-type C57BL/6 mice without ($n = 5$) or with ($n = 5$) anti-IL-17A antibody treatment or IL-17A$^{-/-}$ ($n = 6$) were infected i.p. with 5×10^4 spirochetes of *B. hermsii* strain DAH. Clinical score (*A*) and incidence (*B*) of CNS manifestations were monitored until day 21 post infection. (*C*–*F*) Wild-type C57BL/6 mice without ($n = 5$) or with ($n = 5$) anti-IL-17A antibody treatment or IL-17A$^{-/-}$ ($n = 7$) were infected with 5×10^4 spirochetes of *B. hermsii* strain DAH, euthanized on 14 dpi, and spinal cords were harvested for histological examination of H&E-stained specimens (*C*). mRNA levels of *IL-6*, *IL-8*, and *TNF*-α in spinal cords were determined via qRT-PCR (*D*). Immunofluorescence staining of Iba-1 (green) and CD68 (red) were performed (*E*). Stained sections were scanned on the 3D HISTECH system, followed by analysis of positively stained cells with the Indica laboratory software. The percentage of number of CD68$^+$ cells to Iba-1$^+$ cells were calculated and plotted (*F*). All data are represented as mean ± SD. Where applicable, data were analyzed via two-tailed unpaired Student's *t* test. *$P < 0.05$, **$P < 0.01$, ***$P < 0.001$, and ns means no significant difference ($P \geq 0.05$). (Scale bar for *C* and *E*: 50 μm.)

residing in the spleen. Follow-up studies are required to identify the synergy between IL-17 and IL-6, the source of IL-6, and to test whether IL-6 contributes to the auto amplification loop in the spinal cord during the pathogenesis of RFNB.

IL-17A/F$^{-/-}$ mice show significant variation of gut microbiota and are resistant to autoimmune diseases. Restoration of gut microbes makes animals susceptible to the induction of autoimmunity, suggesting that IL-17 could also induce the neuroinflammation via the regulation of the microbiota (47). In fact, 10–20% of broad-spectrum antibiotics treated Lyme disease patients show post treatment Lyme disease syndrome in the CNS, suggesting that the gut microbiota is involved in the pathogenesis of the LNB (48).

In conclusion, this study demonstrates that IL-17 is involved in the development of RFNB, and after treatment with IL-17A neutralizing antibody, inflammation, and symptoms in CNS of RFNB mice were significantly improved. Therefore, targeting the IL-17 signaling axis may be a promising approach for the treatment of RFNB or possibly other neurological complications associated with the genus *Borrelia*.

Materials and Methods

Mice and Infections. Mice were maintained in a specific pathogen-free facility of the Institute of Medical Biology (IMB), Chinese Academy of Medical Sciences, and housed in individually ventilated cages with free access to food and water. C57BL/6 mice were provided by Department of Experimental Animal of IMB. IL-17A$^{-/-}$ mice were on the C57BL/6 background, with age and sex matched with wild-type C57BL/6 mice and they were provided via Materials Transfer Agreement by the Center for Animal Disease Modeling, Institute of Biomedical Sciences, Tokyo Institute of Technology, Japan. All animal procedures were approved by the Institutional Animal Care and Use Committee of Institute of Medical Biology, Chinese Academy of Medical Science (2015-10). The mice were supplied with hardwood chips as bedding and housed in a temperature-controlled, air-conditioned room on a 12-h light-dark cycle. Eight- to 12-wk-old male or female mice were injected intraperitoneally with 5×10^4 bacteria (in 200 μL PBS) of a fully virulent *B. hermsii* strain DAH, a clinical isolate and blood was sampled on the indicated day post infection from tail vein, and bacteremia was monitored by dark field microscopy. The number of animals used in each group was given in the figure legends.

Neurological manifestations in *B. hermsii*-infected mice were scored daily using a well-established experimental autoimmune encephalomyelitis clinical scoring protocol (49): 0, no observable signs; 1, completely limp tail and/or weakness of one hind limb; 2, weakness of both hind limbs; 3, paralysis of one hind limb; 4, paralysis of both hind limbs; and 5, death related with this disease.

For histopathology and other analysis, mice were euthanized by CO_2, transcardially perfused with PBS, and the spinal cord was harvested at the indicated time points. For treatment with anti-IL-17A neutralizing antibody, a day before *B. hermsii* infection, wild-type C57BL/6 mice were injected intraperitoneally with anti-IL-17A neutralizing antibody (clone: eBioMM17F3, eBioscience) or IgG1 Isotype Control (P3.6.2.8.1, eBioscience) at the dosage of 100 μg for each mouse and repeated treatment on the day 6 and 13 post *B. hermsii* infection.

ELISA for *Borrelia hermsii*-Specific IgM and IgG. *B. hermsii*-specific IgM and IgG were determined as described previously (42, 43). Specific antibody levels were interpreted as ng/μL equivalents using ELISA kits according to the manufacturer's instructions (Bethyl Laboratories).

Multiplex Cytokines Assay. The concentrations of cytokines and chemokines, GM-CSF, IL-6, TNF-α, IL-2, IFN-γ, IL-1β, MIP-1β, IL-13, IL-4, IL-5, IL-17A, MCP-1, IL-10, IL-12 (p70), and IP-10 in serum were determined using Mouse Cytokine/Chemokine Magnetic Bead Panel (Millipore) via Luminex xMAP, according to manufacturer's instructions.

Histopathological Analysis. Tissues were fixed in 10% neutral-buffered formalin for approximately 2 d, followed by a series of standard tissue processing (dehydration, clearing, and wax infiltration) and embedded in paraffin wax. The embedded spinal cord was transversely cut into 2-μm sections for hematoxylin and eosin (H&E) staining and histopathological analysis.

Immunofluorescence Assay. The spinal cord was fixed in 10% neutral-buffered formalin, and then embedded in paraffin for further analysis. Two-micrometer sections were prepared for immunofluorescence (IF) staining. Specific proteins in tissue sections were detected by incubations of properly diluted primary antibodies (anti-ZO-1 Ab, anti-CD31 Ab, anti-CD68 Ab, and anti-Iba1 Ab all from ServiceBio). Following the addition of corresponding fluorescent-conjugated secondary antibodies, the stained sections were counterstained with DAPI and then scanned on the 3D HISTECH system (3DHISTECH). The positive staining was quantified by using the Indica Labs-Highplex FL (v3.1.0) module of Halo software (v3.0.311.314).

Immunohistochemistry Staining. Immunohistochemistry staining of CD68 was performed on sections cut from the paraffin-embedded tissues using anti-CD68 rabbit polyclonal antibody (Servicebio). Antigen retrieval was conducted by microwaving slides in antigen retrieval buffer (pH 6.0) for 8 min at 800 W prior to incubation with anti-CD68 antibody (1:400, Servicebio) at 4 °C overnight, followed by PBS wash and then incubation with HRP-conjugated goat anti-rabbit IgG (1:200, Servicebio) for 50 min at room temperature. The reaction was visualized using the IHC Kit D (Servicebio). The stained sections were scanned on the 3D HISTECH system (3DHISTECH). The Alpathwell software (Servicebio) was used to analyze the positive staining according to the manufacture's instruction. The quantification of CD68 was conducted using modified H-scores ([{% of weak staining} × 1] + [{% of moderate staining} × 2] + [{% of strong staining} × 3]) as described (50), to determine the overall percentage of CD68 positivity across the entire stained sample.

RNA-Seq Analysis. Total RNA was extracted from spinal cord tissues using the TRIzol Plus RNA Purification Kit (Invitrogen). The concentration and purity of total RNA were determined by Qubit3.0 Flurometer (Life Technologies). RNA was enriched and purified via magnetic beads with Oligo (dT). mRNAs were fragmented into short fractions by Fragmentation Buffer and used as templates to synthesize the first complementary DNA (cDNA) strands with random six bases primers, and the second cDNA strand was synthesized by adding Buffer, dNTPs, RNase H, and DNA Polymerase I. After elution and purification, the double-stranded cDNA was treated with terminal repair, base A, and sequencing joint, and then the target fragments were recovered by agarose gel electrophoresis for PCR amplification, to complete the preparation of the entire library. Qubit3.0 was used for preliminary quantification of library that was then diluted to 1 ng/μL. Agilent 2100 was used to detect the insert size of the library. After the insert size met the expectation, Bio-Rad CFX 96 fluorescence quantitative PCR instrument and Bio-Rad Kit iQ SYBR GRN were used for Q-PCR to accurately quantify the effective concentration of the library (the effective concentration of the library >10 nM) to ensure the quality of the library. Qualified libraries were sequenced using Illumina platform. The sequencing strategy was PE150. RNA analysis was performed using R Packages.

qRT-PCR. Total RNA was purified from spinal cord and spleen tissues via the TRIzol Plus RNA Purification Kit (Invitrogen), followed by the removal of genomic DNA via gDNA Eraser (Perfect Real Time) (Takara) synthesis kit. Reverse transcription (RT) was carried out using PrimeScript RT reagent Kit (Takara). Briefly, a total of 500 ng RNA (from spinal cord) or 1 μg RNA (from spleen) was used for each RT. Then qPCR was performed on a CFX96 Touch Real-Time PCR Detection System (Bio-Rad) with 2× TSINGKE Master qPCR Mix-SYBR (+UDG) (TSINGKE) under the following conditions: 50 °C for 2 min, 95 °C for 2 min, and 40 cycles at 95 °C for 15 s and 60 °C for 30 s. The copy number of target RNA was calculated via the comparative Ct (ΔΔCt) method and normalized to the house keeping gene GAPDH. The following primer pairs were used: *Gapdh* 5′-GAG AGTGTTTCCTCGTCCCG-3′ forward and 5′-ACTGTGCCGTTGAATTTGCC-3′ reverse; *Cxcl10* 5′-TCATTTTCTGCCTCATCCTGCT-3′ forward and 5′-TGCGTGGCTTCA-CTCCAGTT-3′ reverse; *Il1b* 5′-TGAAGTTGACGGACCCCAAA-3′ forward and 5′-GAAG-GTCC ACGGGAAAGACA-3′ reverse; *Ccl12* 5′-TAGCTACCACCATCAGTCCTC-3′ forward and 5′-TTAACCCACTTCTCCTTGGGGT-3′ reverse; *Cyp4f18* 5′-CACAGCCTCCCAAACG-AAAC-3′ forward and 5′-ACGGCTTCAGGAAACGGTAG-3′ reverse; *Lcn2* 5′-AATGTC ACC-TCCATCCTGGTC-3′ forward and 5′-GGCGAACTGGTTGTAGTCCG-3′ reverse;

C1ra 5′-AC- ATCACCACAAAAGGCGTG-3′ forward and 5′-ACAGGGTTGACAGGTT TCCC-3′ reverse; *Itga5* 5′-AGGTGACAGGACTCAGCAAC-3′ forward and 5′-AAACA CTTGGCTTCAGGGC-A-3′ reverse; *Ptgs2* 5′-GCATTCTTTGCCCAGCACTT-3′ forward and 5′-TCTCAGGGATGTG-AGGAGGG-3′ reverse; *Tnfaip3* 5′-AGCTCAACTGGTGTCGT-GAA-3′ forward and 5′-CGA-GTGTCGTAGCAAAGTCCT-3′ reverse; *ApLNBBr* 5′-TGG TGTTCCGTTCCACAG-AC-3′ forward and 5′-GGTCACTACAAGCACCACGA-3′ reverse; *Car3* 5′-TGGAGGAGTATGCGGACCTT-3′ forward and 5′-AACACCTGGCTTCATGGGTG-3′ reverse; *Hsd11b1* 5′-GGGAGCCCATG-TGGTATTGA-3′ forward and 5′-GCGAGGTCTGA GTGATGTGG-3′ reverse; *Calca* 5′-GATC-AAGAGTCACCGCTTCG-3′ forward and 5′-GG GCTGCTTTCCAAGATTGA-C-3′ reverse; *Mc5r* 5′-TGGGTCTCGTCAGCCTCTTA-3′ forward and 5′-GATGTACCTGTCCACCGCAA-3′ reverse; *IL6* 5′-AGTTGCCTTCTTGGGACTGA-3′ forward and 5′-CCTCCGACTTGTGAAGT-GGT-3′ reverse; *IL8* 5′-CAGCTGCCTTAACCCC ATCA-3′ forward and 5′-CTTGAGAAGTCC-ATGGCGAAA-3′ reverse; *TNF*-α 5′-GACA AGGCTGCCCCGACTACG-3′ forward and 5′-CTT-GGGGCAGGGGCTCTTGAC-3′ reverse.

Statistical Analysis. Where applicable, a two-tailed unpaired Student's *t* test was performed to compare differences between two groups unless otherwise noted. A P value <0.05 was considered statistically significant, and significance is denoted as * (**$P < 0.01$, ***$P < 0.005$, and ****$P < 0.001$).

Data, Materials, and Software Availability. RNA-seq data have been deposited in National Center for Biotechnology Information (NCBI) BioProject (PRJNA751594) (51).

ACKNOWLEDGMENTS. We thank Dr. Tim Manser and Mr. Darren Dougharty for helping edit the manuscript. This work is supported by the National Natural Science Foundation of China (81571594), Yunnan Key Research and Development Program (202103AQ100001), Yunnan Provincial Key Laboratory of Vector-borne Diseases Control and Research (2015DG037), and Yunnan Organ Transplantation Clinical Medical Center (2020SYZ-Z-024).

Author affiliations: [a]Institute of Medical Biology, Chinese Academy of Medical Sciences and Peking Union Medical College, Kunming, Yunnan 650118, China; and [b]Department of Microbiology and Immunology, Thomas Jefferson University, Philadelphia, PA 19107

1. D. Cadavid, A. G. Barbour, Neuroborreliosis during relapsing fever: Review of the clinical manifestations, pathology, and treatment of infections in humans and experimental animals. *Clin. Infect. Dis.* **26**, 151–164 (1998).
2. U. Koedel, V. Fingerle, H. W. Pfister, Lyme neuroborreliosis-epidemiology, diagnosis and management. *Nat. Rev. Neurol.* **11**, 446–456 (2015).
3. A. C. Steere *et al.*, Lyme borreliosis. *Nat. Rev. Dis. Primers* **2**, 16090 (2016).
4. P. M. Southern Jr., J. P. Sanford, Relapsing fever: A clinical and microbiological review. *Medicine (Baltimore)* **48**, 129–149 (1969).
5. E. Talagrand-Reboul, P. H. Boyer, S. Bergström, L. Vial, N. Boulanger, Relapsing fevers: Neglected tick-borne diseases. *Front. Cell. Infect. Microbiol.* **8**, 98 (2018).
6. L. Ford, D. M. Tufts, Lyme neuroborreliosis: Mechanisms of *B. burgdorferi* infection of the nervous system. *Brain Sci.* **11**, 789 (2021).
7. E. A. Eckman, J. Pacheco-Quinto, A. R. Herdt, J. J. Halperin, Neuroimmunomodulators in neuroborreliosis and Lyme encephalopathy. *Clin. Infect. Dis.* **67**, 80–88 (2018).
8. S. Rauer *et al.*; Consensus group, Guidelines for diagnosis and treatment in neurology - Lyme neuroborreliosis. *Ger. Med. Sci.* **18**, Doc03 (2020).
9. S. Rauer *et al.*, Lyme neuroborreliosis. *Dtsch. Arztebl. Int.* **115**, 751–756 (2018).
10. R. Dersch *et al.*, Efficacy and safety of pharmacological treatments for Lyme neuroborreliosis in children: A systematic review. *BMC Neurol.* **16**, 189 (2016).
11. A. R. Pachner, P. Duray, A. C. Steere, Central nervous system manifestations of Lyme disease. *Arch. Neurol.* **46**, 790–795 (1989).
12. K. Boden, S. Lobenstein, B. Hermann, G. Margos, V. Fingerle, *Borrelia miyamotoi*-associated neuroborreliosis in immunocompromised person. *Emerg. Infect. Dis.* **22**, 1617–1620 (2016).
13. D. Cadavid, D. D. Thomas, R. Crawley, A. G. Barbour, Variability of a bacterial surface protein and disease expression in a possible mouse model of systemic Lyme borreliosis. *J. Exp. Med.* **179**, 631–642 (1994).
14. D. Cadavid, E. Garcia, H. Gelderblom, Coinfection with *Borrelia turicatae* serotype 2 prevents the severe vestibular dysfunction and earlier mortality caused by serotype 1. *J. Infect. Dis.* **195**, 1686–1693 (2007).
15. J. A. Gebbia, J. C. Monco, J. L. Degen, T. H. Bugge, J. L. Benach, The plasminogen activation system enhances brain and heart invasion in murine relapsing fever borreliosis. *J. Clin. Invest.* **103**, 81–87 (1999).
16. J. C. Garcia-Monco, N. S. Miller, P. B. Backenson, P. Anda, J. L. Benach, A mouse model of *Borrelia meningitis* after intradermal injection. *J. Infect. Dis.* **175**, 1243–1245 (1997).
17. H. Liu, D. Fitzgerald, B. Gran, J. M. Leong, K. R. Alugupalli, Induction of distinct neurologic disease manifestations during relapsing fever requires T lymphocytes. *J. Immunol.* **184**, 5859–5864 (2010).
18. O. A. Maximova *et al.*, Virus infection of the CNS disrupts the immune-neural-synaptic axis via induction of pleiotropic gene regulation of host responses. *eLife* **10**, e62273 (2021).
19. H. Singh, A. Singh, A. A. Khan, V. Gupta, Immune mediating molecules and pathogenesis of COVID-19-associated neurological disease. *Microb. Pathog.* **158**, 105023 (2021).
20. S. Najjar *et al.*, Central nervous system complications associated with SARS-CoV-2 infection: Integrative concepts of pathophysiology and case reports. *J. Neuroinflammation* **17**, 231 (2020).
21. J. Milovanovic *et al.*, Interleukin-17 in chronic inflammatory neurological diseases. *Front. Immunol.* **11**, 947 (2020).
22. J. K. Kolls, A. Lindén, Interleukin-17 family members and inflammation. *Immunity* **21**, 467–476 (2004).
23. M. Gelderblom *et al.*, Neutralization of the IL-17 axis diminishes neutrophil invasion and protects from ischemic stroke. *Blood* **120**, 3793–3802 (2012).
24. M. J. McGeachy, D. J. Cua, S. L. Gaffen, The IL-17 family of cytokines in health and disease. *Immunity* **50**, 892–906 (2019).
25. J. Huppert *et al.*, Cellular mechanisms of IL-17-induced blood-brain barrier disruption. *FASEB J.* **24**, 1023–1034 (2010).
26. M. Oosting *et al.*, Borrelia species induce inflammasome activation and IL-17 production through a caspase-1-dependent mechanism. *Eur. J. Immunol.* **41**, 172–181 (2011).
27. A. Pietikäinen *et al.*, Cerebrospinal fluid cytokines in Lyme neuroborreliosis. *J. Neuroinflammation* **13**, 273 (2016).
28. P. Gyllemark, P. Forsberg, J. Ernerudh, A. J. Henningsson, Intrathecal Th17- and B cell-associated cytokine and chemokine responses in relation to clinical outcome in Lyme neuroborreliosis: A large retrospective study. *J. Neuroinflammation* **14**, 27 (2017).
29. T. G. Schwan, B. J. Hinnebusch, Bloodstream- versus tick-associated variants of a relapsing fever bacterium. *Science* **280**, 1938–1940 (1998).
30. A. F. Setiadi *et al.*, IL-17A is associated with the breakdown of the blood-brain barrier in relapsing-remitting multiple sclerosis. *J. Neuroimmunol.* **332**, 147–154 (2019).
31. C. C. John *et al.*, Global research priorities for infections that affect the nervous system. *Nature* **527**, S178–S186 (2015).
32. S. D. Skaper, L. Facci, M. Zusso, P. Giusti, An inflammation-centric view of neurological disease: Beyond the neuron. *Front. Cell. Neurosci.* **12**, 72 (2018).
33. T. Casselli *et al.*, A murine model of Lyme disease demonstrates that Borrelia burgdorferi colonizes the dura mater and induces inflammation in the central nervous system. *PLoS Pathog.* **17**, e1009256 (2021).
34. L. Ellis, M. W. Curtis, S. M. Gunter, J. E. Lopez, Relapsing fever infection manifesting as aseptic meningitis, Texas, USA. *Emerg. Infect. Dis.* **27**, 2681–2685 (2021).
35. S. Majumder, M. J. McGeachy, IL-17 in the pathogenesis of disease: Good intentions gone awry. *Annu. Rev. Immunol.* **39**, 537–556 (2021).
36. A. Chiricozzi, J. G. Krueger, IL-17 targeted therapies for psoriasis. *Expert Opin. Investig. Drugs* **22**, 993–1005 (2013).
37. L. Monin, S. L. Gaffen, Interleukin 17 family cytokines: Signaling mechanisms, biological activities, and therapeutic implications. *Cold Spring Harb. Perspect. Biol.* **10**, a028522 (2018).
38. D. J. Cua, C. M. Tato, Innate IL-17-producing cells: The sentinels of the immune system. *Nat. Rev. Immunol.* **10**, 479–489 (2010).
39. J. Kawanokuchi *et al.*, Production and functions of IL-17 in microglia. *J. Neuroimmunol.* **194**, 54–61 (2008).
40. S. Hu *et al.*, IL-17 production of neutrophils enhances antibacteria ability but promotes arthritis development during *Mycobacterium tuberculosis* infection. *EBioMedicine* **23**, 88–99 (2017).
41. M. M. Curtis, S. S. Way, Interleukin-17 in host defence against bacterial, mycobacterial and fungal pathogens. *Immunology* **126**, 177–185 (2009).
42. K. R. Alugupalli *et al.*, B1b lymphocytes confer T cell-independent long-lasting immunity. *Immunity* **21**, 379–390 (2004).
43. K. R. Alugupalli *et al.*, The resolution of relapsing fever borreliosis requires IgM and is concurrent with expansion of B1b lymphocytes. *J. Immunol.* **170**, 3819–3827 (2003).
44. G. S. Dickinson *et al.*, Toll-like receptor 2 deficiency results in impaired antibody responses and septic shock during *Borrelia hermsii* infection. *Infect. Immun.* **78**, 4579–4588 (2010).
45. P. Muranski, N. P. Restifo, Essentials of Th17 cell commitment and plasticity. *Blood* **121**, 2402–2414 (2013).
46. X. Ma *et al.*, IL-17 enhancement of the IL-6 signaling cascade in astrocytes. *J. Immunol.* **184**, 4898–4906 (2010).
47. T. Regen *et al.*, IL-17 controls central nervous system autoimmunity through the intestinal microbiome. *Sci. Immunol.* **6**, eaaz6563 (2021).
48. M. Morrissette *et al.*, A distinct microbiome signature in posttreatment Lyme disease patients. *mBio* **11**, e02310–e02320 (2020).
49. S. D. Miller, W. J. Karpus, "Experimental autoimmune encephalomyelitis in the mouse" in *Current Protocols in Immunology*, J. E. Coligan, D. H. Margulies, E. M. Shevach, W. Strober, Eds. (Ann Boyle, 2007), pp. 15.1.1–15.1.18.
50. A. Paschalis *et al.*, Prostate-specific membrane antigen heterogeneity and DNA repair defects in prostate cancer. *Eur. Urol.* **76**, 469–478 (2019).
51. M. Cheng *et al.*, Pathogenesis of Neuroborreliosis during Relapsing Fever, accession # PRJNA751594. NCBI BioProject. https://www.ncbi.nlm.nih.gov/bioproject?term=PRJNA751594. Deposited 2 August 2021.